PLOS PATHOGENS

RESEARCH ARTICLE

Bps polysaccharide of *Bordetella pertussis* resists antimicrobial peptides by functioning as a dual surface shield and decoy and converts *Escherichia coli* into a respiratory pathogen

Audra R. Fullen[1], Jessica L. Gutierrez-Ferman[1], Kacy S. Yount[1], Cheraton F. Love[2], Hyun G. Choi[1], Mario A. Vargas[3], Deepa Raju[3], Kara N. Corps[4], P. Lynne Howell[3,5], Purnima Dubey[1], Rajendar Deora [1,6]*

1 The Department of Microbial Infection and Immunity, The Ohio State University Wexner Medical Center, Columbus, Ohio, United States of America, 2 Department of Microbiology and Immunology, Wake Forest University Health Sciences, Winston-Salem, North Carolina, United States of America, 3 Program in Molecular Medicine, The Hospital for Sick Children, Toronto, Ontario, Canada, 4 Department of Veterinary Biosciences, Comparative Pathology and Digital Imaging Shared Resource, The Ohio State University Comprehensive Cancer Center, Columbus, Ohio, United States of America, 5 Department of Biochemistry, University of Toronto, Toronto, Ontario, Canada, 6 Department of Microbiology, The Ohio State University, Columbus, Ohio, United States of America

* Rajendar.deora@osumc.edu

Abstract

Infections and disease caused by the obligate human pathogen *Bordetella pertussis* (*Bp*) are increasing, despite widespread vaccinations. The current acellular pertussis vaccines remain ineffective against nasopharyngeal colonization, carriage, and transmission. In this work, we tested the hypothesis that Bordetella polysaccharide (Bps), a member of the poly-β-1,6-*N*-acetyl-D-glucosamine (PNAG/PGA) family of polysaccharides promotes respiratory tract colonization of *Bp* by resisting killing by antimicrobial peptides (AMPs). Genetic deletion of the *bpsA-D* locus, as well as treatment with the specific glycoside hydrolase Dispersin B, increased susceptibility to AMP-mediated killing. Bps was found to be both cell surface-associated and released during laboratory growth and mouse infections. Addition of bacterial supernatants containing Bps and purified Bps increased *B. pertussis* resistance to AMPs. By utilizing ELISA, immunoblot and flow cytometry assays, we show that Bps functions as a dual surface shield and decoy. Co-inoculation of C57BL/6J mice with a Bps-proficient strain enhanced respiratory tract survival of the Bps-deficient strain. In combination, the presented results highlight the critical role of Bps as a central driver of *B. pertussis* pathogenesis. Heterologous production of Bps in a non-pathogenic *E. coli* K12 strain increased AMP resistance *in vitro*, and augmented bacterial survival and pathology in the mouse respiratory tract. These studies can serve as a foundation for other PNAG/PGA polysaccharides and for the development of an effective *Bp* vaccine that includes Bps.

Author summary

Pertussis or whooping cough, caused by the obligate human pathogen *Bordetella pertussis* (*Bp*), is resurging in many countries. Currently, the mechanism by which *B. pertussis* subverts and resists host immunity is poorly known. In this manuscript, we examined the role of the *B. pertussis* polysaccharide Bps in promoting resistance to antimicrobial peptides (AMPs), a critical component of host immune defense. We show that the presence of Bps on the bacterial cell surface enhanced AMP resistance. Bps was released both during bacterial growth and during mouse infections. We further found that Bps functioned both as a surface shield and decoy, thereby inhibiting AMP binding. Simultaneous infection of mice with Bps-proficient and Bps-deficient strains resulted in greater survival of the Bps-deficient strain in the mouse respiratory tract. Finally, production of Bps in a non-pathogenic *E. coli* strain increased AMP resistance *in vitro*, and increased bacterial survival and heightened pathology in the mouse respiratory tract. Our study provides new insights into how *B. pertussis* has evolved to survive in the mammalian respiratory tract.

Introduction

Bordetella pertussis (*Bp*) is a strict human-adapted Gram-negative respiratory tract pathogen, which causes whooping cough or pertussis, a highly contagious disease. Despite high and widespread vaccine coverage, the incidence of pertussis has increased in many countries. Pertussis is traditionally described as a childhood disease, which results in severe and sometimes fatal infections in newborns and infants. There has also been an increase in infections of vaccinated adolescents and adults, in whom pertussis manifests as a persistent cough with milder symptoms [1–4].

The adaptation of *Bp* to humans as an exclusive host was primarily associated with extensive loss of genomic content and gene inactivation [4,5]. Thus, *Bp* is likely evolving to retain only genes required for its survival in human hosts. The *bpsA-D* locus, which encodes the *Bordetella* polysaccharide (Bps), is conserved in all sequenced and annotated strains of *Bp*. Therefore, investigating pathogenic roles of Bps will provide insights into how *Bp* survives in its only niche, the human respiratory tract. Bps belongs to the poly-β-1,6-*N*-acetyl-D-glucosamine (PNAG/PGA) family of polysaccharides. These polysaccharides are produced by numerous Gram-positive and Gram-negative bacteria, fungal and eukaryotic organisms including *Plasmodia* spp., the causative agents of malaria [6–9]. For *Bp*, Bps was the first identified factor to promote colonization of the mouse nose. In addition, Bps was also critical for the colonization of the mouse trachea and lungs [6]. However, the mechanism(s) by which Bps promotes respiratory tract survival is unclear.

After exposure to inhaled microorganisms, the innate immune system of the respiratory tract functions as a highly effective defense against infectious agents. Antimicrobial peptides (AMPs) are critical innate immune components within the respiratory tract which exhibit broad-spectrum and potent microbicidal activities against both Gram-negative and Gram-positive bacteria [10–12]. However, bacteria employ diverse strategies to resist killing by AMPs. Alterations of net charge and permeability of the cell surface are some commonly employed strategies for AMP resistance. Common bacterial factors in Gram-negative and Gram-positive bacteria that contribute to AMP resistance are LPS and teichoic acids (TA), respectively [13–15]. There are few reported mechanisms that detail how *Bp* resists human AMPs. Modification of the lipo-oligosaccharide lipid A region with glucosamine increases resistance against LL-37 [16]. Similar to that observed for TA of Gram-positive bacteria and LPS of *V. cholerae* [15,17–

19], we described that the addition of the amino acid D-alanine to a yet unidentified outer membrane component enhances resistance to several human AMPs [20].

In the current manuscript, we tested the hypothesis that Bps promotes resistance of *Bp* to AMPs. We show that Bps binds AMPs and protects bacteria from AMP-mediated killing when present on the bacterial surface and as a secreted factor. We also investigated the pathogenic consequences of Bps production in a non-pathogenic commensal *E. coli* K12 strain. Production of Bps as the sole *Bp* factor was sufficient to confer on *E. coli* the ability to survive in the mouse respiratory tract and resulted in aggravated lung pathology.

Results

The *bpsA-D* polysaccharide locus of *B. pertussis* contributes to AMP resistance

We showed previously that a *Bp* strain harboring an in-frame deletion in the genes of the *bpsA-D* locus (Δ*bpsA-D*), which encodes the Bps polysaccharide, colonized the mouse respiratory tract less efficiently than the wildtype (WT) strain as early as six hours post-challenge [6]. Since AMPs act early after infection to protect the respiratory tract from bacterial pathogens, we hypothesized that the Δ*bpsA-D* strain will be more sensitive to these antibacterial compounds than the WT strain. We first compared the sensitivities of these two strains to polymyxin B (PmB), a cationic antibiotic peptide that is an excellent model for bactericidal actions of AMPs [21]. Compared to the WT strain, the Δ*bpsA-D* mutant was significantly more sensitive to PmB-mediated killing (Fig 1A). Complementation of the Δ*bpsA-D* mutant with the plasmid pMM11 containing the cloned *bpsA-D* locus (Δ*bpsA-D*^{comp}) considerably increased bacterial survival in the presence of PmB when compared to that of the mutant strain harboring the vector plasmid only (Δ*bpsA-D*^{vec}) (Fig 1A).

Next, we tested the sensitivities of the WT and Δ*bpsA-D* strains to human AMPs. We used LL-37 (a human cathelicidin produced by phagocytes and epithelial cells in the respiratory tract) [22] along with HNP-1 and HNP-2 (members of α-defensin family found in the human respiratory tract) [23,24]. Compared to the WT strain, the Δ*bpsA-D* mutant was killed significantly better in the presence of all these host AMPs (Fig 1B–1D). Furthermore, Δ*bpsA-D*^{comp} strain showed significantly more resistance compared to the Δ*bpsA-D*^{vec} strain when exposed to each AMP (Fig 1B–1D). Interestingly, compared to the WT bacteria, complementation of the Δ*bpsA-D* strain with pMM11 resulted in increased resistance to PmB and LL-37 (Fig 1A–1B), which could largely be because the Δ*bpsA-D*^{comp} strain produces higher amounts of Bps than WT bacteria (S1 Fig). Taken together, these results demonstrate that the *bpsA-D* locus promotes resistance to several different AMPs.

Dispersin B increases the susceptibility of *B. pertussis* to PmB and LL-37

Dispersin B (DspB) is a glycoside hydrolase that specifically hydrolyzes poly-β-1,6-N-acetyl-D-glucosamines [25–27]. While the exact structure of Bps is unknown, based on its immune reactivity and susceptibility to DspB, Bps appears to be a poly-β-1-6-N-acetyl-D-glucosamine polysaccharide [6,27,28]. Thus, DspB offers a useful biochemical tool to assess the contribution of Bps to AMP resistance independent of the Δ*bpsA-D* strain. The WT and Δ*bpsA-D* strains were treated with various concentrations of DspB before incubation with PmB or LL-37. Based on the results in Fig 2A, 50 μg/ml of DspB was chosen for further experiments, since it reduced the levels of detectable Bps on WT bacteria to that detectable on Δ*bpsA-D* bacteria. The residual detectable material in the Δ*bpsA-D* strain probably represents some other material that is weakly cross-reactive with WGA-HRP. Compared to incubation with PmB or LL-37 alone,
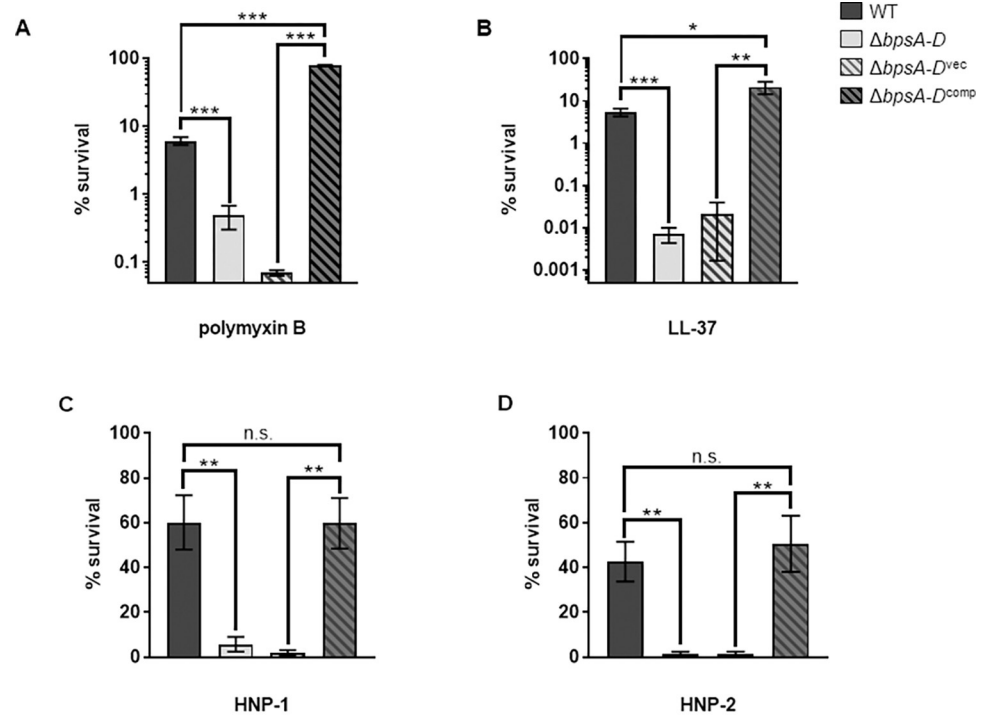
Fig 1. Bps promotes resistance to antimicrobial peptides. Survival of WT, Δ*bpsA-D*, Δ*bpsA-D*vec, and Δ*bpsA-D*comp in the presence of .5 μg/ml polymyxin B (a), .5 μg/ml LL-37 (b), 50 μg/ml HNP-1 (c), and 50 μg/ml HNP-2 (d). Bacteria were exposed to the indicated concentrations of AMPs in 10mM Na_3PO_4 for 2 hours. Each data point represents the mean and s.e.m. of triplicates from one experiment and is representative of at least three independent experiments. Statistical differences were assessed by unpaired two-tailed Student's *t* test. *, $p < 0.05$; **, $p < 0.005$; ***, $p < 0.0005$. n.s. not significant.

treatment of the WT strain with either DspB + PmB (Fig 2B) or DspB + LL-37 (Fig 2C) resulted in a 3.5- and 3.0-log-fold increase in bacterial killing, respectively. Compared to treatment with PmB or LL-37 alone, treatment of the Δ*bpsA-D* strain with DspB + PmB (Fig 2B) or DspB + LL-37 (Fig 2C) did not result in any further increase in bacterial killing, suggesting that the activity of DspB is specific to Bps. Treatment with DspB alone did not have any significant effect on the survival of either the WT or Δ*bpsA-D* strains (S2A Fig), suggesting that DspB does not have any toxic effect on *Bp*. Furthermore, treatment with heat-inactivated DspB before exposure to LL-37 had no significant reduction in survival compared to bacteria treated with LL-37 alone (S2B Fig). These data show that enzymatic degradation of Bps increases the susceptibility of *Bp* to killing by PmB and LL-37.

The presence of Bps on the *B. pertussis* cell surface inhibits LL-37 and PmB binding

Since the results presented thus far suggest that Bps protects *Bp* by limiting the killing activity of PmB and LL-37, we hypothesized that Bps inhibits the binding of AMP to the bacterial cell surface. To test this, we used flow cytometry to quantify the binding of FITC-labelled LL-37 to fixed bacteria. Fig 3A shows overlaid histograms comparing median fluorescence intensities of FITC, which are quantified in Fig 3B. Addition of FITC-labeled LL-37 to WT bacteria resulted in an increase in FITC fluorescence compared to control (WT bacteria alone), indicating that LL-37 binds to WT bacteria. Addition of FITC-labeled LL-37 to Δ*bpsA-D* bacteria led to a
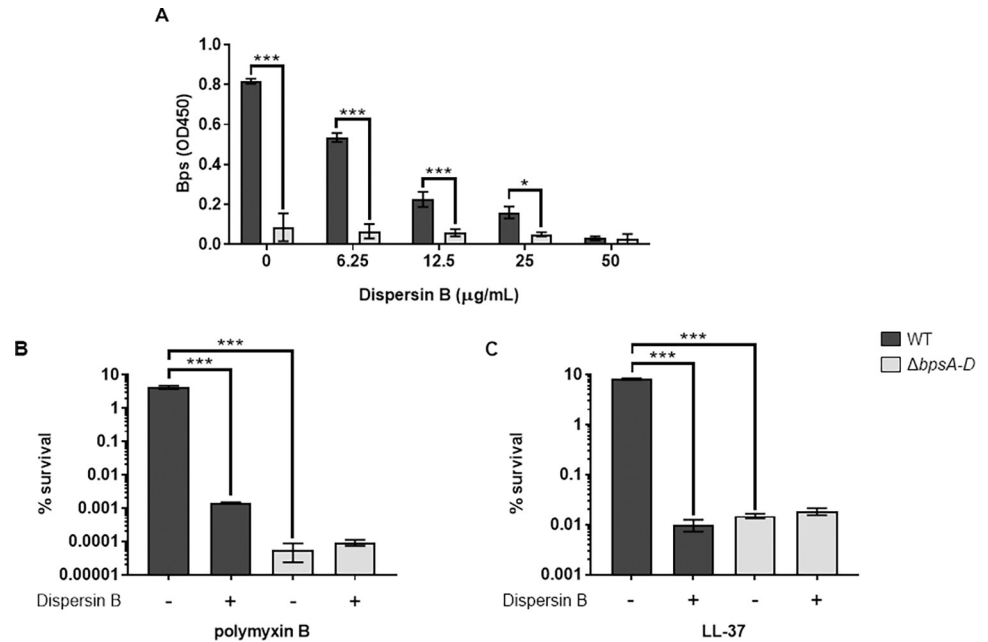
Fig 2. Dispersin B hydrolyzes Bps and increases the susceptibility of *B. pertussis* to PmB and LL-37. (a) Bps was quantified by ELISA from the WT or Δ*bpsA-D* strains following incubation with indicated concentrations of Dispersin B. Each data point represents the mean and s.e.m. of triplicates from one experiment and is representative of two independent experiments. Statistical differences were assessed by two-way ANOVA. *, $p<0.05$; ***, $p<0.0005$. (b, c) Survival of WT and Δ*bpsA-D* strains following treatment with 50 μg/ml Dispersin B or buffer in the presence of .5 μg/ml polymyxin B (b) or .5 μg/ml LL-37 (c). Each data point represents the mean and s.e.m. of triplicates from one experiment and is representative of two independent experiments. Statistical differences were assessed by one-way ANOVA. ***, $p<0.0005$.

considerable increase in FITC fluorescence, suggesting that higher amounts of LL-37 bind to the Δ*bpsA-D* strain than to the WT strain. This phenotype was also observed with PmB, using an ELISA-based method with an α-PmB antibody. As shown in S3 Fig, PmB bound to WT bacteria, indicated by an increase in signal compared to the negative control (blank). However,
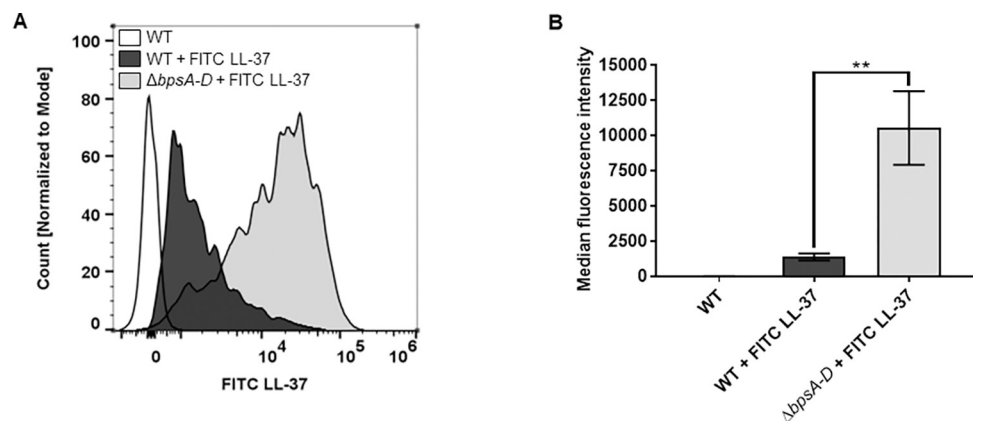
Fig 3. The presence of Bps on the cell surface inhibits LL-37 binding. (a, b) Bacteria were fixed and exposed to FITC-labeled LL-37 followed by measurement of the fluorescence intensity of FITC-labeled LL-37 bound to bacteria by flow cytometry. (a) Bacterial counts for each strain were normalized to mode. (b) Median fluorescence intensities were quantified and assessed for statistical analysis. Data represent triplicates from one of two independent experiments. Statistical differences were assessed by one-way ANOVA. **, $p<0.005$.

addition of PmB to Δ*bpsA-D* bacteria resulted in an increase in signal compared to the WT bacteria (S3 Fig). These results suggest that the presence of Bps on the *Bp* cell surface reduces the binding of PmB and LL-37, providing one explanation for reduced AMP-mediated killing of WT bacteria.

Bps is released during laboratory growth of *B. pertussis*

In addition to producing polysaccharides on the cell surface, many bacteria also release them in the growth medium [8,29]. It is not known if Bps is naturally released during laboratory growth of *Bp*. To determine this, the amounts of Bps present on the bacterial cell surface (cell-associated) and released into the growth medium (supernatant; collected after centrifugation and filtration of the spent medium) were quantitated by ELISA using the lectin wheat germ agglutinin (WGA) conjugated to HRP. In WT cells, Bps was detected on both the cell surface and in the supernatant (Fig 4A). As expected, negligible amounts of Bps were detected on the cell-surface or in supernatant obtained from the Δ*bpsA-D* strain. These results demonstrate that *Bp* releases Bps during laboratory growth.

Cell-free Bps increases the resistance of *B. pertussis* to AMPs

Next, we determined if Bps released into the culture medium would increase AMP resistance. First, WT bacteria were incubated with PmB in the presence of SS media or filtered supernatants from either the WT or Δ*bpsA-D* bacteria. Compared to the addition of either SS media or supernatant from the Δ*bpsA-D* strain (Δ*bpsA-D* sup), addition of supernatant from the WT
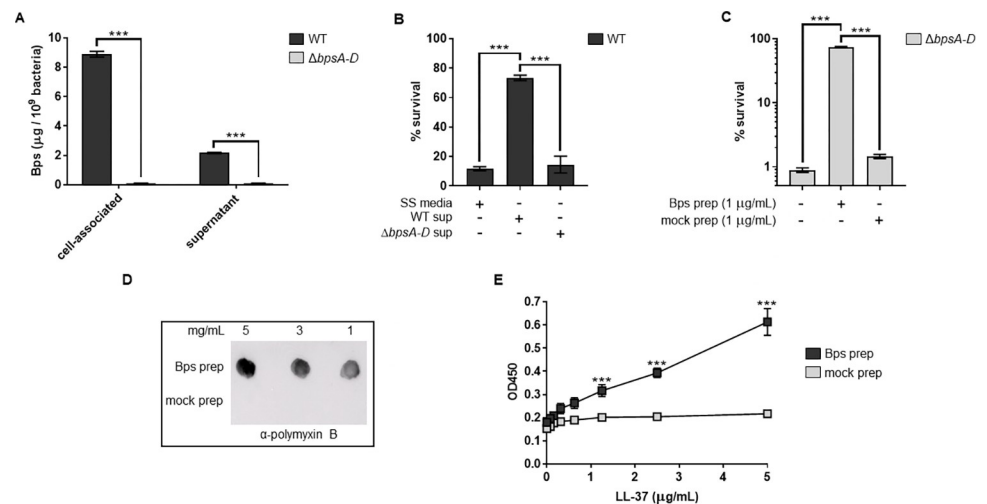
Fig 4. *B. pertussis* releases Bps during laboratory growth, and cell-free Bps provides protection from and binds to PmB and LL-37. (a) Quantitation of cell-associated and released (supernatant) Bps from the WT and Δ*bpsA-D* strains by ELISA. Each data point represents the mean and s.e.m. of eight wells from one experiment and is representative of two independent experiments. Statistical differences were assessed by two-way ANOVA. ***, $p < 0.0005$. (b, c) Survival of WT and Δ*bpsA-D* strains in the presence of PmB (b) or LL-37 (c). Supernatants from WT and the Δ*bpsA-D* cultures (b) or purified Bps and mock preparation (c) were added as indicated. Each data point represents the mean and s.e.m. of triplicates from one experiment and is representative of two independent experiments. Statistical differences were assessed by one-way ANOVA. ***, $p < 0.0005$. (d, e) Bps binds PmB and LL-37. (d) Bps or mock preparations were spotted on nitrocellulose membranes. To detect PmB binding, the membranes were incubated with PmB, washed and probed with α-polymyxin B antibody conjugated to HRP. (e) Binding of Bps or mock preparations to LL-37 was quantified by ELISA using WGA conjugated to HRP. Asterisks indicate significance compared to mock prep. Each data point represents the mean and s.e.m. from one experiment and is representative of two independent experiments. Statistical differences between Bps and mock preps were assessed by unpaired two-tailed Student's *t* test. ***, $p < 0.0005$.

strain (WT sup) resulted in enhanced survival of the WT strain by PmB (Fig 4B). We also tested if Bps purified from bacterial cells would increase bacterial survival. Addition of purified Bps (Bps prep) increased survival of the Δ*bpsA-D* bacteria in the presence of LL-37. In contrast, addition of a mock-purified preparation from the Δ*bpsA-D* strain did not have any significant effect on the survival of the Δ*bpsA-D* strain (Fig 4C). Collectively, these results suggest that the addition of cell-free Bps increases AMP resistance of *Bp*.'

Cell-free Bps binds to PmB and LL-37

We used immunoblotting and ELISA to test whether cell-free Bps bound PmB and LL-37, respectively. For immunoblots, different amounts of Bps prep or mock prep were spotted on a nitrocellulose membrane, followed by incubation with PmB. After extensive washing, the bound PmB was detected by incubation with a mouse α-PmB primary antibody followed by a goat α-mouse HRP-conjugated secondary antibody. PmB bound to the Bps prep but not to the mock prep (Fig 4D). Similarly, LL-37 bound to Bps in a dose-dependent manner as detected by ELISA, whereas the mock prep showed very weak binding which did not increase with increasing amounts of LL-37 (Fig 4E). Collectively, these results suggest that cell-free Bps limits the killing activity of AMPs by binding to them.

Presence of the WT strain increases resistance to LL-37-mediated killing *in vitro* and promotes respiratory tract survival of the Δ*bpsA-D* strain

Based on the finding that cell-free Bps protects against AMP-mediated killing, we hypothesized that the WT strain will protect the Δ*bpsA-D* strain from AMP-mediated killing. To test this *in vitro*, we incubated monocultures or co-cultures (1:1) of the two strains with LL-37 and enumerated CFUs. When incubated with the WT strain, the susceptibility of the Δ*bpsA-D* strain to LL-37 was nearly identical to that of the WT strain (Fig 5A).
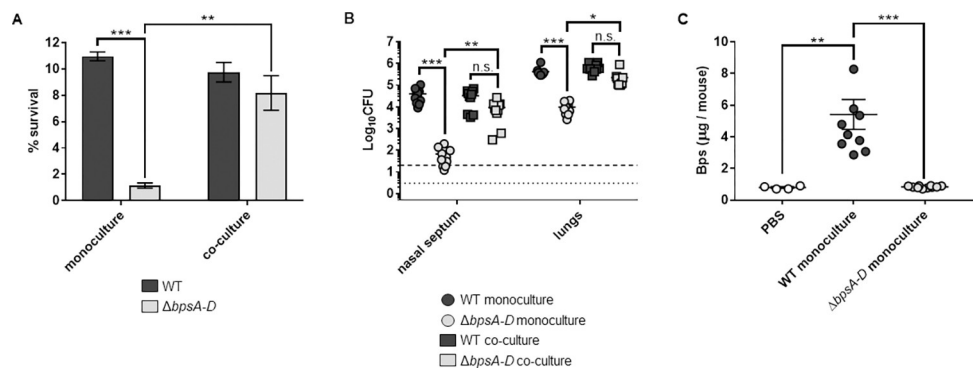
Fig 5. The presence of the WT strain increases Δ*bpsA-D* resistance to LL-37 *in vitro* and enhances its survival in the mouse respiratory tract and Bps is released in mouse lungs during infection. (a) Survival of WT and Δ*bpsA-D* strains either in monoculture or in a 1:1 co-culture of both strains against LL-37. Each data point represents the mean and s.e.m. of triplicates from one of five independent experiments. Statistical differences were assessed by two-way ANOVA. **, p<0.005; ***, p<0.0005. n.s. not significant. (b) Bacterial CFUs recovered from the nasal septum and lungs of C57BL/6J mice four days after aerosol infection with WT or Δ*bpsA-D* in monoculture or in a 1:1 co-culture. Bars indicate the mean and s.e.m. of ten mice. Data from two independent experiments with groups of five mice each are shown. Statistical differences were assessed by two-way ANOVA. *, p<0.05; **, p<0.005; ***, p<0.0005; n.s., not significant. Dotted line represents the lower limit of detection for nasal septum, and dashed line represents the lower limit of detection for lungs. (c) Amounts of Bps in supernatants of lung lysates obtained from mice either instilled with PBS (blank circles) or infected with the indicated strains was quantified by ELISA using WGA conjugated to HRP. For infected mice, bars indicate the mean and s.e.m. of two independent experiments consisting of groups of five mice each (from Fig 5B). For PBS-instilled mice, bars indicate the mean and s.e.m. of one experiment consisting of four mice. Statistical differences were assessed by one-way ANOVA. **, p<0.005; ***, p<0.0005.

https://doi.org/10.1371/journal.ppat.1010764.g005

We then tested if a similar survival advantage will exist for the Δ*bpsA-D* mutant in the mouse respiratory tract when co-infected with the WT strain. C57BL/6J mice were infected by aerosol exposure with the WT or the Δ*bpsA-D* strain either as single strains or when combined in a 1:1 ratio. Bacterial burden was determined by enumeration of CFUs from the nasal septum and lungs at four days post-challenge. Enumeration of CFUs approximately 30 minutes after aerosol challenge confirmed that similar numbers of the two strains were delivered into the nose and the lungs (S4 Fig). Mice infected with only the Δ*bpsA-D* strain (gray circles) harbored significantly lower bacterial burden on the nasal septum and in the lungs compared to mice infected with the WT strain alone (black circles) (Fig 5B). This result is consistent with our previously published results using the intranasal challenge route [6]. Strikingly, when co-infected with the WT strain, the bacterial burden of the Δ*bpsA-D* strain (grey squares) on the nasal septum and in the lungs was similar to that of the WT strain (black squares; Fig 5B). These results indicate that the presence of the WT strain supports the colonization of the Δ*bpsA-D* strain in the mouse nose and lungs.

B. pertussis releases Bps in the mouse lungs

Lung lysates collected from mice were centrifuged and filtered, followed by quantification of Bps in the supernatants by ELISA. Bps was detected in lung supernatants of mice infected with the WT strain (black circles; Fig 5C). In comparison, Bps levels in the lung lysates of mice infected with the Δ*bpsA-D* strain (gray circles) were similar to those of mice instilled only with PBS (clear circles). We speculate that this background level of Bps reactivity is due to the cross-reactivity of the WGA with host carbohydrates [30]. These results suggest that Bps released from the WT strain contributes to the increased bacterial burden of the Δ*bpsA-D* strain in the mouse respiratory tract.

Production of Bps in *E. coli* confers resistance to PmB and LL-37, enhances bacterial survival in the mouse respiratory tract, and augments pathology in the lungs

We then tested whether Bps as the sole *Bordetella* factor was sufficient to provide resistance to AMP-mediated killing in *E. coli*. Since *E. coli* harbors the *pga* locus (a polysaccharide locus with high sequence homology to the *bpsA-D* locus [28], we utilized a derivative of MG1655 (*E. coli* K12 strain) that lacks this locus. This strain was named ARF001. The pMM11 plasmid which encodes Bps was transformed into ARF001 [31–34]. Compared to the strain containing the empty vector (ARF001^vec), the strain containing pMM11 (ARF001^*bpsA-D*) survived better in the presence of PmB (Fig 6A) and LL-37 (Fig 6B). We also confirmed using FITC-labeled LL-37 that production of Bps in *E. coli* inhibited AMP binding (Fig 6C–6D). These results suggest that Bps confers resistance to PmB and LL-37 in *E. coli* independent of other *Bp* factors by inhibiting their binding.

C57BL/6 mice were infected utilizing both intranasal and aerosol routes [35] with either the ARF001^vec or ARF001^*bpsA-D* strain and CFUs were enumerated from the nasal septum and lungs four days post-challenge. Compared to mice infected with the ARF001^vec strain, mice intranasally infected with the ARF001^*bpsA-D* strain had approximately 100- and 400-fold higher bacterial burden in the nasal septum and lungs, respectively (Fig 6E). Upon infection of mice by the aerosol route, the ARF001^vec bacteria were recovered from the nasal septum of only one mouse at the lower limit of detection (3 CFUs) (Fig 6F). No bacteria were recovered from the lungs of any of the mice infected by aerosol. This suggests that ARF001^vec strain is unable to survive in the mouse nose and lungs when infected by the aerosol route. In comparison, the ARF001^*bpsA-D* bacteria were recovered from the nasal septum when infected by the aerosol
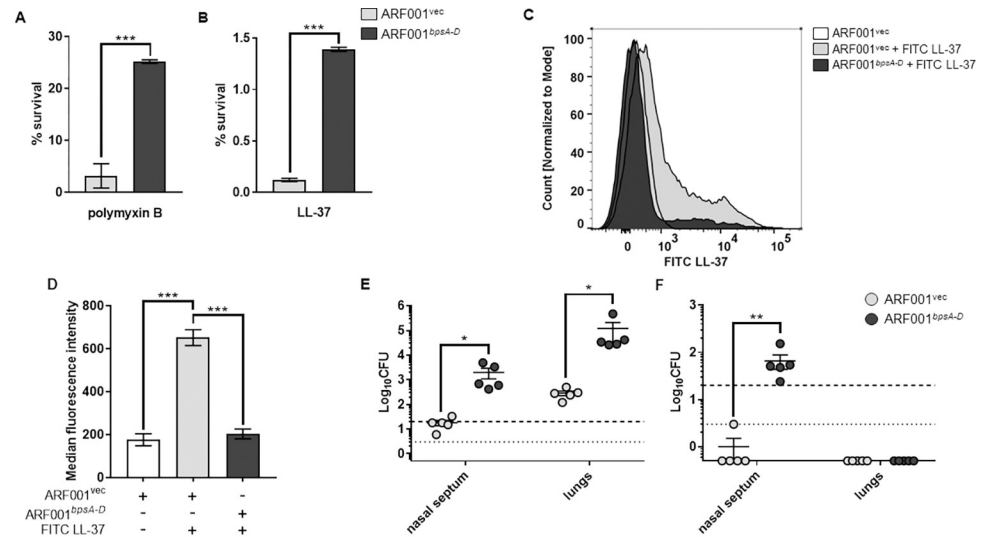
Fig 6. Bps enhances PmB and LL-37 resistance, inhibits AMP binding, and promotes respiratory tract survival when produced in *E. coli*. (a, b) Survival of ARF001^{vec} and ARF001^{bpsA-D} strains in the presence of .5 μg/ml polymyxin B (a) or .5 μg/ml of LL-37 (b). Bacteria were exposed to the indicated concentrations of AMPs for 2 hours in 10mM Na$_3$PO$_4$ buffer. Each data point represents the mean and s.e.m. of triplicates from one of two independent experiments. Statistical differences were assessed by unpaired two-tailed Student's *t* test. *, p<0.05; ***, p<0.0005. (c, d) Binding of FITC LL-37 to the ARF001^{vec} or ARF001^{bpsA-D} strains was measured by flow cytometry. Bacteria were fixed and exposed to FITC-labeled LL-37 and then the fluorescence intensity of FITC-labeled LL-37 bound to bacteria was measured by flow cytometry. (c) Bacterial counts for each strain were normalized to mode. (d) Median fluorescence intensities were quantified and assessed for statistical analysis. Data represent triplicates from one of two independent experiments. Statistical differences were assessed by one-way ANOVA. ***, p<0.0005. (e, f) Bacterial CFUs recovered from the nasal septum and lungs three days after intranasal challenge (e) or one day after aerosol challenge (f) with either the ARF001^{vec} or ARF001^{bpsA-D} strains. Bars indicate the mean and s.e.m. of groups of five mice each. Data are representative of one of two independent experiments with five mice each. Statistical differences were determined by unpaired two-tailed Student's *t* test for each organ. *, p<0.05; **, p<0.005. Dotted line represents the lower limit of detection for nasal septum, and dashed line represents the lower limit of detection for lungs.

https://doi.org/10.1371/journal.ppat.1010764.g006

route (Fig 6F). The observed decrease in colonization in the nasal septum and lungs after aerosol infection was not due to the inability of bacteria to reach these sites as enumeration of CFUs approximately 30 minutes after aerosol infection resulted in the recovery of both the ARF001^{vec} and ARF001^{bpsA-D} strains from the nasal septum and lungs (S5A Fig). However, the number of bacteria recovered 30 minutes after aerosol infection was lower than that recovered 30 minutes after intranasal infection (S5B Fig), explaining the differences in bacterial burden between intranasal and aerosol infections.

Evaluation and semi-quantitative lesion scoring performed on lungs from mice intranasally infected with ARF001^{vec} (Fig 7A–7D) strain revealed mild neutrophilic interstitial pneumonia, mild to moderate thickening of the pulmonary interstitium, and moderate numbers of neutrophils infiltrating the interstitium and bronchioles. In contrast, lungs from mice infected ARF001^{bpsA-D} (Fig 7E–7H) were characterized by a marked neutrophilic and macrophagic pneumonia with significant regional consolidation and thickening of the interstitium. In central areas of consolidation, very large numbers of neutrophils and macrophages obscured the distinction between alveoli and interstitium, and multifocally, alveolar walls were lined by hyperplastic type II pneumocytes, a common pulmonary response to injury. BALT was similarly expanded in this group of lungs adjacent to bronchioles. Degeneration and necrosis, edema, and hemorrhage were similar in all examined lung specimens. Total histopathology scores from mice infected with ARF001^{bpsA-D} were significantly higher than total scores from
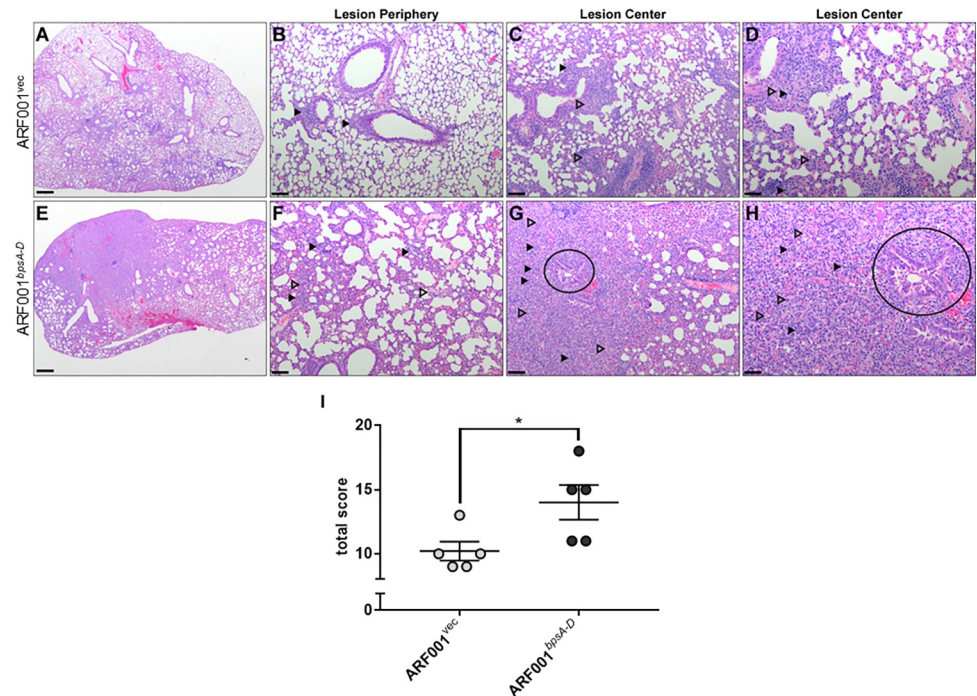
Fig 7. Bps converts *E. coli* to a respiratory pathogen in C57BL/6 mice. Pulmonary infection with *E. coli* expressing *bpsA-D* results in severe pneumonia (e-h) compared to *E. coli* expressing the empty vector (a-d). ARF001^{bpsA-D}-infected mice: Neutrophils (filled arrows) admixed with edema (open arrows) at lesion periphery (f) and large numbers of neutrophils (filled arrows), macrophages (open arrows) with bronchiolar epithelial hyperplasia, dysplasia and necrosis (circle) at lesion center (g, h). ARF001^{vec}-infected mice: few mixed leukocytes (arrows) at lesion periphery (b) and multifocal, small numbers of neutrophils (closed arrow) and moderate numbers of macrophages (open arrow) around bronchioles (c, d). Scale bar in a, e = 500 μm, 20x total magnification; Scale bar in b, c, f, g = 100 μm, 100x total magnification; Scale bar in d, h = 50 μm, 200x total magnification.

mice infected with ARF001^{vec} (Fig 7I). Taken together, these results suggest that the production of Bps in *E. coli* is sufficient to impart the ability to colonize the mouse respiratory tract and induce pathology in the lungs.

Discussion

Successful prevention of microbial infection and disease necessitates a deeper understanding of the mechanisms by which microorganisms avoid host immunity. AMPs constitute a major component of the first line of immune defense in the mammalian respiratory tract. However, the respiratory pathogen *Bp* multiplies rapidly upon natural human infection and experimental infection of laboratory animals and is thus capable of overcoming these defenses [36,37]. In this manuscript, we investigated the role of the Bps polysaccharide in protecting *Bp* against AMP-mediated killing. We demonstrated that compared to the WT strain, the isogenic Δ*bpsA-D* mutant strain was more sensitive to PmB and several structurally diverse human AMPs. Treatment of the WT strain by DspB, a glycoside hydrolase that specifically cleaves Bps, also enhanced AMP sensitivity. Consistent with a positive role for Bps in AMP resistance, overproduction of Bps in the Δ*bpsA-D* strain by utilizing multiple copy plasmid complementation enhanced resistance to both PmB and LL-37. The pathogenic impact of elevated production of Bps in Bp is currently under investigation.

We have discovered two different strategies by which Bps confers resistance to AMPs. First, we demonstrated that while the WT strain bound PmB and LL-37, the Δ*bpsA-D* mutant strain

bound relatively higher amounts of these AMPs. Because of high affinity for LPS, interaction of AMPs with the gram-negative bacterial surface results in the displacement of the divalent cations (Ca_2^+ and Mg_2^+) that bind to the phosphate groups of the inner core of LPS. Because of their bulky nature, AMP binding then results in destabilization of the bacterial membrane [38]. In *B. bronchiseptica* and other bacteria, the LPS O-antigen promotes AMP resistance by limiting the interaction of AMPs with the bacterial surface [39,40]. Unlike *B. bronchiseptica*, *Bp* does not produce O-antigen [41]. We propose that in the absence of the O-antigen, Bps functions to inhibit AMP interaction with LPS and blocks their bactericidal effects. PNAG/PGA polysaccharides contain variable amounts of de-*N*-acetylated glucosamine residues, rendering these polymers positively charged [8,42,43]. The deacetylation status of Bps is not known. Previously, the PIA polysaccharide of *Staphylococcus epidermidis* was shown to protect against killing by LL-37, and it was suggested that electrostatic repulsion is a likely mechanism of this protection [42]. A similar mechanism can also be hypothesized for cell-associated Bps.

Second, we report that *Bp* releases Bps both in the medium during laboratory growth and in mouse lungs during infection. Incubation with both naturally released and purified Bps increased the resistance of bacterial cells to PmB and LL-37. Cell-free Bps bound to both PmB and LL-37. This suggests that cell-free Bps can sequester/trap AMPs by functioning as a sink and thereby neutralize their bactericidal activity. This property of Bps resembles that of decoy receptors found in mammalian systems, which bind specific growth factors or cytokines [44,45]. Rather than signaling or activating the receptor complex this binding resulted in inhibition because the signaling molecules were trapped and rendered inactive. While many PNAG polysaccharides are released during laboratory growth [8,42,43], this is the first time a naturally released member of the PNAG polysaccharide family has been found to be released during infection and to mediate protection against a host immune component by functioning as a decoy.

The dual shielding and decoy effect of Bps reported in this manuscript appears somewhat paradoxical. How can a polysaccharide simultaneously inhibit AMP binding in one form and promote binding in another form? A previous study investigated the conformations of a series of linear and cyclic oligosaccharides related to PNAG. Linear oligosaccharides were not rigid and adopted several different conformations. The cyclic di-, tri, and tetra-saccharides adopted a symmetrical flattened ring conformation whereas the larger cyclic oligosaccharides were characterized by complicated shapes, resembling twisted rings [46]. It is possible that conformational differences exist between cell-associated and cell-free Bps resulting in variable effects on AMP binding. We propose that the binding of AMPs to Bps and other PNAG polysaccharides is dependent on its cellular location and conformation and involves various molecular forces including ionic forces.

Previously when inoculated intranasally with single strains and compared to the WT strain, the Δ*bpsA-D* strain survived at considerably lower numbers in the mouse respiratory tract [6]. In the current report, we obtained similar results when mice were infected with single strains using the aerosol route. Further, we observed that when mice were infected by the aerosol route with a 1:1 mixture of the WT and Δ*bpsA-D* strains, the numbers of the mutant strain harvested from the nasal septum and lungs were similar to that of the WT strain. We also observed increased survival of the mutant strain when incubated with LL-37 in the presence of the WT strain. We propose that Bps released by the WT strain in the mouse respiratory tract can sequester AMPs and is a major contributor to the enhanced survival of the mutant strain in the presence of the WT strain. Additionally, as evident from our AMP binding data, a proportion of AMPs could also be sequestered by binding to Bps on the cell surface of WT cells.

Production of Bps as a single *Bp* virulence factor in a laboratory-derived non-pathogenic *E. coli* strain conferred the ability to resist killing by PmB and LL-37. Like that observed in *Bp*,

production of Bps inhibited AMP binding to *E. coli*. Production of Bps also increased the survival of *E. coli* in the mouse nose when mice were infected by the aerosol route, and in both the nose and lungs when infected by the intranasal route. Histological analyses of the lungs showed marked enhancement of pathology when mice were intranasally infected with the Bps-producing *E. coli* strain. We consider these findings to be quite striking, since continuous laboratory passage and culturing of *E. coli* has led to several genetic mutations, deletions, and loss of surface structures resulting in a non-pathogenic organism which is not suited to a life inside the host or outside a laboratory [47,48]. Furthermore, *E. coli* is rarely considered to be a respiratory bacterium, as most pulmonary infections by *E. coli* are a result of dissemination from the gastrointestinal or urinary tract and from oropharyngeal aspirations [49].

In conclusion, Bps promotes resistance against AMP-mediated killing of *Bp* by functioning as a dual surface shield and decoy. The current findings further corroborate Bps as a principal determinant of *Bp* virulence and should serve as a model for investigating the pathogenic roles of other PNAG polysaccharides, which are conserved in many microbial species. Since Bps is not a component of current acellular pertussis vaccines, a vaccine containing Bps could control the resurgence of pertussis. Finally, Bps is a rare bacterial factor in that it confers virulence by itself in animal models of infection.

Materials and methods

Ethics statement

Housing, husbandry, and experiments with animals were carried out in accordance with the guidelines approved by the Institutional Animal Care and Use Committee of The Ohio State University. C57BL/6J mice (Jackson; male and female, 6 to 12 weeks old) were bred in-house. All experiments were reviewed and approved by The Ohio State University Institutional Animal Care and Use Committee (Protocols #2017A00000090 and #2021A00000069).

Bacterial growth conditions

Bacterial strains and plasmids used in this study are listed in S1 Table. *Bp* strains were maintained on Bordet-Gengou (BG) agar supplemented with 10% defibrinated sheep blood (Hemo-Stat, Laboratories, Dixon, CA) at 37˚C for four days. For liquid cultures, *Bp* strains were grown in Stainer-Scholte (SS) broth supplemented with 0.1 mg/ml of heptakis (2,6-di-*O*-methyl-β-cyclodextrin, Sigma Aldrich, St. Louis, MO, USA) [20,50,51] at 37˚C in a roller drum (80 rpm). *E. coli* strains were grown on either Luria-Bertani (LB) agar or in LB broth. As necessary, growth medium was supplemented with the appropriate antibiotics: chloramphenicol (Cm), 10 μg/ml; streptomycin (Sm), 100 μg/ml; and nalidixic acid (Nal), 20 μg/ml.

Antimicrobial peptide killing assays

Bp and *E. coli* strains were grown to an OD_{600} = 1.0 in SS or LB broth, respectively. Bacterial cells were harvested by centrifugation (13,500 rpm, 5 minutes), washed twice with sterile PBS, and resuspended in 10mM sodium phosphate buffer (pH 7.0). Dilutions of AMPs were prepared in 10mM sodium phosphate buffer, and bacterial cells were incubated with indicated concentrations of AMPs rotating at 37˚C for 2 hours. CFUs were enumerated by spotting 10 μl of 10-fold serial dilutions onto BG agar plates with Sm (*Bp*) or LB agar plates (*E. coli*) with Cm. Percent survival was determined by dividing the number of CFUs recovered after AMP treatment by the number of CFUs recovered from only buffer added controls.

For co-culture killing assays, WT and Δ*bpsA-D* strains were mixed in a ratio of 1:1 in 10mM sodium phosphate buffer (pH 7.0) and incubated with LL-37 at 37˚C rotating for 2

hours. We recently discovered that while the WT strain is resistant to both streptomycin and nalidixic acid, absence of the *bpsA-D* locus results in sensitivity to nalidixic acid (S6 Fig). Therefore, we took advantage of the differential sensitivities of the two strains to nalidixic acid to track their survival in co-culture experiments. Bacterial suspensions were plated on both BG agar with Sm (to enumerate both WT and Δ*bpsA-D* strains) and BG agar with Nal (to enumerate only the WT strain). CFUs of Δ*bpsA-D* strain were calculated by subtracting the counts obtained on BG agar with Nal from the counts obtained on BG agar with Sm.

To determine the role of spent culture supernatant in AMP protection, bacteria grown to an $OD_{600} = 1.0$ in SS medium were pelleted by centrifugation (13,500 rpm, 5 minutes). After adjustment of pH to 7.4, the culture supernatants were filtered through a .22 μm filter (Millipore, catalog no. SCGP0052) and stored at -20°C. Bacteria were resuspended in either culture supernatants or SS broth. Bps prep or mock prep were purified as previously described [6]. AMP killing assays with *E. coli* strains were done under the same conditions as with *Bp*, and bacteria were enumerated on LB agar with Cm. For all AMP killing assays, at least two independent experiments were performed with n = 3.

Quantification of Bps by ELISA

Bp strains were grown to $OD_{600} = 1.0$, harvested by centrifugation (13,500 rpm, 15 minutes), washed with sterile 1X PBS twice and resuspended in sterile 1X PBS. To quantify cell-associated Bps, 1×10^8 CFUs in 100 μl of PBS were incubated overnight at 4°C in 96-well plates (Corning, NY), washed three times with PBST (Tween 20) followed by blocking with 5% milk at 37°C for 1 hour. After washing three more times with PBST, the plates were incubated with wheat germ agglutinin (WGA) conjugated to horseradish peroxidase (HRP) (Biotium Inc. Hayward, CA, USA) at a dilution of 1:1000. After incubation at 37°C for 1 hour followed by five washes with PBST, 100 μl of 3,3',5,5'-tetramethylbenzidine (TMB, Sigma Aldrich, St. Louis, MO, USA) were added to each well. The reaction was stopped using 100μl of 1M H_2SO_4.

To quantify released Bps, 1 ml of bacterial culture corresponding to $OD_{600} = 1.0$ was centrifuged (13,500 rpm, 15 minutes). Then, the supernatant was carefully aliquoted, filtered through a .22 μm filter (Millipore, catalog no. SCGP00525), and stored at -20°C for later use. 100 μl of supernatants were added to each well of 96-well plates and the plates incubated overnight at 4°C. ELISA assays were performed as described above. Six independent experiments were performed with n = 8.

To quantitate Bps from mouse lungs, homogenized lung lysates (for preparation of mouse lung lysates, please see below) from PBS-inoculated or *Bp*-infected mice were centrifuged (5000 rpm, 5 minutes), the supernatant carefully aliquoted, filtered through a .22 μm filter, and stored at -20°C for later use. 300 μl of supernatants were added to each well of 96-well plates and Bps was quantitated by ELISA as described above. Two independent experiments were performed with n = 5.

Dispersin B treatment

Dispersin B (DspB) was purified as previously described [27]. Bacterial cells corresponding to $OD_{600} = 1.0$ were harvested by centrifugation (13,500 rpm 5 minutes), washed twice with 1X PBS, and resuspended in DspB buffer (20mM Tris base, pH 8.0; 500mM NaCl). DspB treatments were carried out with 1×10^8 CFUs at indicated concentrations by incubating at 37°C rotating for 2 hours. DspB was heat-inactivated via incubation at 56°C for 30 minutes. The effect of DspB on cell-associated Bps was quantified by ELISA as described above. To perform AMP killing assays after treatment with DspB, bacteria were washed twice with 1X PBS, then

resuspended in 10mM sodium phosphate buffer and incubated with indicated concentrations of AMPs. Two independent AMP killing assays were performed in technical triplicate.

Binding of LL-37 to bacteria by flow cytometry

Bacteria were harvested by centrifugation (13,500, 5 minutes), washed and fixed in 4% paraformaldehyde (PFA) with overnight rotation at 4˚C. Cells were then washed with PBS, blocked with 1% BSA and probed with 1mM FITC-labelled LL-37 overnight rotating at 4˚C. After two washes with PBS, approximately 10,000 events were collected per sample by using a Cytek Aurora Flow Cytometer (Cytek, Fremont, CA). FloJo software was used for data analysis. Two independent experiments were performed with n = 3.

Binding of PmB to bacteria by ELISA

Bacteria were harvested by centrifugation (13,500, 5 minutes), washed, fixed in 4% paraformaldehyde (PFA), then coated on high-binding 96-well plates (Corning, NY) and incubated at 4˚C overnight. Next, plates were washed three times with PBST, blocked with 5% milk, and probed with 10 µg/ml polymyxin B at 4˚C overnight. Next, mouse monoclonal anti-polymyxin B antibody (ab40014) (Abcam) was added at a dilution of 1:1000 for one hour followed by three washes with PBST. The HRP-conjugated secondary antibody was added at a dilution of 1:1000. After incubation at 37˚C for 1 hour followed by five washes with PBST, 100 µl of 3,3',5,5'-tetramethylbenzidine (TMB, Sigma Aldrich, St. Louis, MO, USA) were added to each well. The reaction was stopped using 100µl of 1M H_2SO_4. Two independent experiments were performed with n = 3.

Binding of AMPs to purified Bps

Serial dilutions of LL-37 were coated on high-binding 96-well plates (Corning, NY) and incubated at 4˚C overnight. Next, plates were washed three times, blocked with 5% milk, and probed with 50 µg/ml Bps and a mock preparation as described [6]. WGA conjugated to HRP (Biotium) was used to quantify the amount of Bps bound to LL-37 by ELISA as described above. Two independent experiments were performed with n = 6.

For PmB binding, 10 µl of 1:2, 1:5 and 1:10 dilutions of 10 mg/ml stock of purified Bps preparations or mock preparations strain were spotted on a nitrocellulose membrane and allowed to dry overnight. The membrane was blocked in 5% milk for 30 minutes followed by incubation with 25 µg/ml of PmB for one hour. Next, mouse monoclonal anti-polymyxin B antibody (ab40014) (Abcam) was added at a dilution of 1:1000 for one hour followed by three washes with TBST. The HRP-conjugated secondary antibody was added at a dilution of 1:5000 for one hour, followed by three washes with TBST and detection by the ECL system.

Mouse models of infection

Male and female C57BL/6J (Jackson) mice were used for all experiments. For all mouse experiments, two independent experiments were performed with groups of five mice. For aerosol infection, mice were infected with 10^8 CFU/ml of *Bp* WT or Δ*bpsA-D* either in monoculture or mixed in a 1:1 ratio, *E. coli* ARF001[vec] or ARF001[bpsA-D] in monoculture, or PBS as a negative control in an Allied Schuco S5000 Nebulizer for 30 minutes. A cohort of infected mice was sacrificed within 30 minutes after aerosol infection to determine the initial bacterial burden. After designated times post-challenge, the nasal septum and lungs were harvested, mechanically disrupted in PBS + 1% casein using hand-held homogenizers [52], and *Bp* counts were enumerated on BG agar plates with Sm for single strain inoculum or by plating separately on BG agar

with Sm and BG agar with Nal as described above. For mice infected with *E. coli* strains, CFUs were enumerated by plating on LB agar with Cm. No bacterial colonies were recovered from mice that were administered PBS.

For intranasal infection with *E. coli*, 5×10^7 CFUs in 50 μl (1X PBS) were intranasally administered to each mouse. A cohort of infected mice was sacrificed within 30 minutes after aerosol infection to determine the initial bacterial burden. After 3 days, the nasal septum and lungs were harvested from each mouse and bacterial counts were enumerated by plating LB agar with Cm.

A board-certified comparative pathologist (Dr. Corps) performed blinded semi-quantitative lesion scoring on n = 5 lungs infected with *E. coli* strains and routinely stained with hematoxylin and eosin. Semi-quantitative lesion scores addressed the following parameters (S2 Table) and were devised based on numerous previously published methodologies and in reflection of lesions present in the experimental cohort: degree of cellularity and consolidation of lung tissue as a percent of total tissue; thickness of alveolar walls; degeneration or necrosis in any portion of the examined lung; presence of edema; presence of hemorrhage; percent of examined alveolar and interstitial tissue infiltrated by neutrophils; percent of bronchioles infiltrated by neutrophils; percent of examined alveoli distant to the lesion center containing alveolar macrophages; and perivascular or peribronchiolar expansion of lymphoid populations +/- plasma cells (bronchioalveolar lymphoid tissue, BALT).

Statistics

Statistical analyses of results were performed by unpaired two tailed t-test, one-way ANOVA, two-way ANOVA and Bonferroni posttest. All statistical analyses were performed using GraphPad Prism 7.05.

Supporting information

S1 Fig. Δ*bpsA-D*^comp^ strain produces higher amounts of Bps than WT strain. Quantitation of Bps from WT, Δ*bpsA-D*, Δ*bpsA-D*^vec^, and Δ*bpsA-D*^comp^ strains by ELISA. Each data point represents the mean and s.e.m. of n = 10 from one experiment and is representative of three independent experiments. Statistical differences were assessed by two-way ANOVA. ***, p<0.0005.
(TIF)

S2 Fig. Dispersin B has no significant effect on the survival of *Bp*. (a) Survival of WT and Δ*bpsA-D* strains after incubation for 2 hours with Dispersin B at 37˚C. Each data point represents the mean and s.e.m. of triplicates from one experiment and is representative of two independent experiments. Statistical differences were assessed by unpaired two-tailed Student's *t* test. (b) Survival of WT bacteria following treatment with PBS, 50 μg/ml Dispersin B, or 50 μg/ml heat-inactivated Dispersin B in the presence of .5 μg/ml LL-37. Dispersin B was inactivated by incubation at 56˚C for 30 minutes. Each data point represents the mean and s.e.m. of triplicates from one experiment and is representative of two independent experiments. Statistical differences were assessed by one-way ANOVA. **, p<0.005; ***, p<0.0005.
(TIF)

S3 Fig. The presence of Bps on the cell surface inhibits PmB binding. Binding of polymyxin B to WT and Δ*bpsA-D* strains was determined by ELISA utilizing a mouse monoclonal anti-polymyxin B antibody, as described in the Materials and Methods. Blank designates wells where PBS was added instead of bacterial cells. Each data point represents the mean and s.e.m. of triplicates from one of two experiments. Statistical differences were assessed by one-way

ANOVA. *, p<0.05; **, p<0.005; ***, p<0.0005.
(TIF)

S4 Fig. Bacterial CFUs recovered from the nasal septum and lungs of mice 30 minutes after aerosol infection with *Bp*. Bacterial CFUs recovered from the nasal septum and lungs of C57BL/6J mice 30 minutes after aerosol infection with co-culture of WT and Δ*bpsA-D* strain in a 1:1 ratio. Bars indicate the mean and s.e.m. of groups of five mice each. Data are representative of one of two independent experiments. Statistical differences were assessed by two-tailed Student's *t* test for each organ. Dotted line represents the lower limit of detection for nasal septum, and dashed line represents the lower limit of detection for lungs.
(TIF)

S5 Fig. Bacterial CFUs recovered from the nasal septum and lungs of mice 30 minutes after aerosol or intranasal infection with *E. coli* strains. Bacterial CFUs recovered from the nasal septum and lungs 30 minutes after aerosol (a) or intranasal (b) challenge with either the ARF001^{vec} or ARF001^{bpsA-D} strains. Bars indicate the mean and s.e.m. of groups of five mice each. Data are representative of one of two independent experiments. Statistical differences were determined by unpaired two-tailed Student's *t* test for each organ. Dotted line represents the lower limit of detection for nasal septum, and dashed line represents the lower limit of detection for lungs.
(TIF)

S6 Fig. Bacterial growth on nalidixic acid. WT and Δ*bpsA-D* strains were streaked on BG agar supplemented with 10% defibrinated sheep blood and 20 μg/ml nalidixic acid. Plates were incubated at 37˚C for four days.
(TIF)

S1 Table. Strains and Plasmids.
(DOCX)

S2 Table. Histopathological Scoring Parameters.
(DOCX)

Author Contributions

Conceptualization: Audra R. Fullen, Jessica L. Gutierrez-Ferman, Kacy S. Yount, Cheraton F. Love, Kara N. Corps, Rajendar Deora.

Formal analysis: Audra R. Fullen, Jessica L. Gutierrez-Ferman, Kacy S. Yount, Cheraton F. Love, Kara N. Corps, Rajendar Deora.

Funding acquisition: Kara N. Corps, P. Lynne Howell, Purnima Dubey, Rajendar Deora.

Investigation: Audra R. Fullen, Jessica L. Gutierrez-Ferman, Kacy S. Yount, Cheraton F. Love, Hyun G. Choi, Mario A. Vargas, Deepa Raju, Kara N. Corps.

Methodology: Audra R. Fullen, Jessica L. Gutierrez-Ferman, Kacy S. Yount, Cheraton F. Love, Kara N. Corps, Rajendar Deora.

Project administration: Kara N. Corps, P. Lynne Howell, Purnima Dubey, Rajendar Deora.

Resources: Kara N. Corps, P. Lynne Howell, Purnima Dubey, Rajendar Deora.

Supervision: Kara N. Corps, P. Lynne Howell, Purnima Dubey, Rajendar Deora.

Validation: Audra R. Fullen, Jessica L. Gutierrez-Ferman, Kacy S. Yount, Cheraton F. Love, Kara N. Corps, Rajendar Deora.

Visualization: Audra R. Fullen, Jessica L. Gutierrez-Ferman, Kacy S. Yount, Cheraton F. Love, Kara N. Corps, Rajendar Deora.

Writing – original draft: Audra R. Fullen, Jessica L. Gutierrez-Ferman, Kacy S. Yount, Kara N. Corps, P. Lynne Howell, Rajendar Deora.

Writing – review & editing: Audra R. Fullen, Rajendar Deora.

References

1. Fullen AR, Yount KS, Dubey P, Deora R. Whoop! There it is: The surprising resurgence of pertussis. PLoS Pathog. 2020; 16(7):e1008625. Epub 2020/07/24. https://doi.org/10.1371/journal.ppat.1008625 PMID: 32702023; PubMed Central PMCID: PMC7377359.

2. Dorji D, Mooi F, Yantorno O, Deora R, Graham RM, Mukkur TK. Bordetella Pertussis virulence factors in the continuing evolution of whooping cough vaccines for improved performance. Med Microbiol Immunol. 2018; 207(1):3–26. Epub 2017/11/23. https://doi.org/10.1007/s00430-017-0524-z PMID: 29164393.

3. Dubois V, Locht C. Mucosal Immunization Against Pertussis: Lessons From the Past and Perspectives. Front Immunol. 2021; 12:701285. Epub 2021/07/03. https://doi.org/10.3389/fimmu.2021.701285 PMID: 34211481; PubMed Central PMCID: PMC8239240.

4. Belcher T, Dubois V, Rivera-Millot A, Locht C, Jacob-Dubuisson F. Pathogenicity and virulence of Bordetella pertussis and its adaptation to its strictly human host. Virulence. 2021; 12(1):2608–32. Epub 2021/10/01. https://doi.org/10.1080/21505594.2021.1980987 PMID: 34590541.

5. Bowden KE, Weigand MR, Peng Y, Cassiday PK, Sammons S, Knipe K, et al. Genome Structural Diversity among 31 Bordetella pertussis Isolates from Two Recent U.S. Whooping Cough Statewide Epidemics. mSphere. 2016; 1(3). Epub 2016/06/16. https://doi.org/10.1128/mSphere.00036-16 PMID: 27303739; PubMed Central PMCID: PMC4888882.

6. Conover MS, Sloan GP, Love CF, Sukumar N, Deora R. The Bps polysaccharide of Bordetella pertussis promotes colonization and biofilm formation in the nose by functioning as an adhesin. Mol Microbiol. 2010; 77(6):1439–55. Epub 2010/07/17. MMI7297 [pii] https://doi.org/10.1111/j.1365-2958.2010.07297.x PMID: 20633227.

7. Skurnik D, Cywes-Bentley C, Pier GB. The exceptionally broad-based potential of active and passive vaccination targeting the conserved microbial surface polysaccharide PNAG. Expert Rev Vaccines. 2016; 15(8):1041–53. Epub 2016/02/27. https://doi.org/10.1586/14760584.2016.1159135 PMID: 26918288; PubMed Central PMCID: PMC4985264.

8. Whitney JC, Howell PL. Synthase-dependent exopolysaccharide secretion in Gram-negative bacteria. Trends Microbiol. 2013; 21(2):63–72. Epub 2012/11/03. https://doi.org/10.1016/j.tim.2012.10.001 PMID: 23117123; PubMed Central PMCID: PMC4113494.

9. Cywes-Bentley C, Skurnik D, Zaidi T, Roux D, Deoliveira RB, Garrett WS, et al. Antibody to a conserved antigenic target is protective against diverse prokaryotic and eukaryotic pathogens. Proc Natl Acad Sci U S A. 2013; 110(24):E2209–18. Epub 2013/05/30. https://doi.org/10.1073/pnas.1303573110 PMID: 23716675; PubMed Central PMCID: PMC3683766.

10. Brown KL, Hancock RE. Cationic host defense (antimicrobial) peptides. Curr Opin Immunol. 2006; 18 (1):24–30. Epub 2005/12/13. https://doi.org/10.1016/j.coi.2005.11.004 PMID: 16337365.

11. Lai Y, Gallo RL. AMPed up immunity: how antimicrobial peptides have multiple roles in immune defense. Trends Immunol. 2009; 30(3):131–41. Epub 2009/02/17. S1471-4906(09)00005-2 [pii] https://doi.org/10.1016/j.it.2008.12.003 PMID: 19217824.

12. Geitani R, Moubareck CA, Xu Z, Karam Sarkis D, Touqui L. Expression and Roles of Antimicrobial Peptides in Innate Defense of Airway Mucosa: Potential Implication in Cystic Fibrosis. Front Immunol. 2020; 11:1198. Epub 2020/07/23. https://doi.org/10.3389/fimmu.2020.01198 PMID: 32695100; PubMed Central PMCID: PMC7338688.

13. Joo HS, Fu CI, Otto M. Bacterial strategies of resistance to antimicrobial peptides. Philos Trans R Soc Lond B Biol Sci. 2016; 371(1695). Epub 2016/05/11. https://doi.org/10.1098/rstb.2015.0292 PMID: 27160595; PubMed Central PMCID: PMC4874390.

14. Cole JN, Nizet V. Bacterial Evasion of Host Antimicrobial Peptide Defenses. Microbiol Spectr. 2016; 4 (1). Epub 2016/03/22. https://doi.org/10.1128/microbiolspec.VMBF-0006-2015 PMID: 26999396; PubMed Central PMCID: PMC4804471.

15. Hankins JV, Madsen JA, Giles DK, Brodbelt JS, Trent MS. Amino acid addition to Vibrio cholerae LPS establishes a link between surface remodeling in gram-positive and gram-negative bacteria. Proc Natl Acad Sci U S A. 2012; 109(22):8722–7. https://doi.org/10.1073/pnas.1201313109 PMID: 22589301.

16. Shah NR, Hancock RE, Fernandez RC. Bordetella pertussis Lipid A Glucosamine Modification Confers Resistance to Cationic Antimicrobial Peptides and Increases Resistance to Outer Membrane Perturbation. Antimicrob Agents Chemother. 2014. Epub 2014/05/29. AAC.02590-14 [pii] https://doi.org/10.1128/AAC.02590-14 PMID: 24867963.

17. Abi Khattar Z, Rejasse A, Destoumieux-Garzon D, Escoubas JM, Sanchis V, Lereclus D, et al. The dlt operon of Bacillus cereus is required for resistance to cationic antimicrobial peptides and for virulence in insects. J Bacteriol. 2009; 191(22):7063–73. Epub 2009/09/22. https://doi.org/10.1128/JB.00892-09 [pii] PMID: 19767427.

18. Perego M, Glaser P, Minutello A, Strauch MA, Leopold K, Fischer W. Incorporation of D-alanine into lipoteichoic acid and wall teichoic acid in Bacillus subtilis. Identification of genes and regulation. J Biol Chem. 1995; 270(26):15598–606. https://doi.org/10.1074/jbc.270.26.15598 PMID: 7797557.

19. McBride SM, Sonenshein AL. The dlt operon confers resistance to cationic antimicrobial peptides in Clostridium difficile. Microbiology. 2011; 157(Pt 5):1457–65. Epub 2011/02/19. mic.0.045997–0 [pii] https://doi.org/10.1099/mic.0.045997-0 PMID: 21330441.

20. Taneja NK, Ganguly T, Bakaletz LO, Nelson KJ, Dubey P, Poole LB, et al. D-alanine modification of a protease-susceptible outer membrane component by the Bordetella pertussis dra locus promotes resistance to antimicrobial peptides and polymorphonuclear leukocyte-mediated killing. J Bacteriol. 2013; 195(22):5102–11. https://doi.org/10.1128/JB.00510-13 PMID: 24013634; PubMed Central PMCID: PMC3811601.

21. Srinivas P, Rivard K. Polymyxin Resistance in Gram-negative Pathogens. Curr Infect Dis Rep. 2017; 19 (11):38. Epub 2017/09/13. https://doi.org/10.1007/s11908-017-0596-3 PMID: 28895051.

22. Ridyard KE, Overhage J. The Potential of Human Peptide LL-37 as an Antimicrobial and Anti-Biofilm Agent. Antibiotics (Basel). 2021; 10(6). Epub 2021/06/03. https://doi.org/10.3390/antibiotics10060650 PMID: 34072318; PubMed Central PMCID: PMC8227053.

23. Ganz T. Defensins: antimicrobial peptides of innate immunity. Nat Rev Immunol. 2003; 3(9):710–20. Epub 2003/09/02. https://doi.org/10.1038/nri1180 nri1180 [pii]. PMID: 12949495.

24. Selsted ME, Ouellette AJ. Mammalian defensins in the antimicrobial immune response. Nat Immunol. 2005; 6(6):551–7. Epub 2005/05/24. https://doi.org/10.1038/ni1206 [pii] PMID: 15908936.

25. Ramasubbu N, Thomas LM, Ragunath C, Kaplan JB. Structural analysis of dispersin B, a biofilm-releasing glycoside hydrolase from the periodontopathogen Actinobacillus actinomycetemcomitans. J Mol Biol. 2005; 349(3):475–86. Epub 2005/05/10. S0022-2836(05)00384-0 [pii] https://doi.org/10.1016/j.jmb.2005.03.082 PMID: 15878175.

26. Fekete A, Borbas A, Gyemant G, Kandra L, Fazekas E, Ramasubbu N, et al. Synthesis of beta-(1—>6)-linked N-acetyl-D-glucosamine oligosaccharide substrates and their hydrolysis by Dispersin B. Carbohydr Res. 2011; 346(12):1445–53. Epub 2011/04/13. https://doi.org/10.1016/j.carres.2011.03.029 PMID: 21482420; PubMed Central PMCID: PMC6118123.

27. Little DJ, Pfoh R, Le Mauff F, Bamford NC, Notte C, Baker P, et al. PgaB orthologues contain a glycoside hydrolase domain that cleaves deacetylated poly-beta(1,6)-N-acetylglucosamine and can disrupt bacterial biofilms. PLoS Pathog. 2018; 14(4):e1006998. Epub 2018/04/24. https://doi.org/10.1371/journal.ppat.1006998 PMID: 29684093; PubMed Central PMCID: PMC5933820.

28. Parise G, Mishra M, Itoh Y, Romeo T, Deora R. Role of a putative polysaccharide locus in Bordetella biofilm development. J Bacteriol. 2007; 189(3):750–60. Epub 2006/11/23. https://doi.org/10.1128/JB.00953-06 [pii] PMID: 17114249.

29. Franklin MJ, Nivens DE, Weadge JT, Howell PL. Biosynthesis of the Pseudomonas aeruginosa Extracellular Polysaccharides, Alginate, Pel, and Psl. Front Microbiol. 2011; 2:167. Epub 2011/10/13. https://doi.org/10.3389/fmicb.2011.00167 PMID: 21991261; PubMed Central PMCID: PMC3159412.

30. Castells MT, Ballesta J, Madrid JF, Aviles M, Martinez-Menarguez JA. Characterization of glycoconjugates in developing rat respiratory system by means of conventional and lectin histochemistry. Histochemistry. 1991; 95(4):419–26. Epub 1991/01/01. https://doi.org/10.1007/BF00266971 PMID: 2022492.

31. Itoh Y, Rice JD, Goller C, Pannuri A, Taylor J, Meisner J, et al. Roles of pgaABCD genes in synthesis, modification, and export of the Escherichia coli biofilm adhesin poly-beta-1,6-N-acetyl-D-glucosamine. J Bacteriol. 2008; 190(10):3670–80. Epub 2008/03/25. https://doi.org/10.1128/JB.01920-07 [pii] PMID: 18359807.

32. Ganguly T, Johnson JB, Kock ND, Parks GD, Deora R. The Bordetella pertussis Bps polysaccharide enhances lung colonization by conferring protection from complement-mediated killing. Cell Microbiol. 2014; 16(7):1105–18. Epub 2014/01/21. https://doi.org/10.1111/cmi.12264 PMID: 24438122.

33. Wang X, Preston JF 3rd, Romeo T. The pgaABCD locus of Escherichia coli promotes the synthesis of a polysaccharide adhesin required for biofilm formation. J Bacteriol. 2004; 186(9):2724–34. Epub 2004/04/20. https://doi.org/10.1128/JB.186.9.2724-2734.2004 PMID: 15090514.

34. Kovach ME, Phillips RW, Elzer PH, Roop RM 2nd, Peterson KM. pBBR1MCS: a broad-host-range cloning vector. Biotechniques. 1994; 16(5):800–2. Epub 1994/05/01. PMID: 8068328.

35. Mills KH, Gerdts V. Mouse and pig models for studies of natural and vaccine-induced immunity to Bordetella pertussis. J Infect Dis. 2014; 209 Suppl 1:S16–9. https://doi.org/10.1093/infdis/jit488 PMID: 24626866.

36. Merkel TJ, Halperin SA. Nonhuman primate and human challenge models of pertussis. J Infect Dis. 2014; 209 Suppl 1:S20–3. Epub 2014/03/15. jit493 [pii] https://doi.org/10.1093/infdis/jit493 PMID: 24626867.

37. Higgs R, Higgins SC, Ross PJ, Mills KH. Immunity to the respiratory pathogen Bordetella pertussis. Mucosal Immunol. 2012; 5(5):485–500. Epub 2012/06/22. https://doi.org/10.1038/mi.2012.54 [pii] PMID: 22718262.

38. Mahlapuu M, Hakansson J, Ringstad L, Bjorn C. Antimicrobial Peptides: An Emerging Category of Therapeutic Agents. Front Cell Infect Microbiol. 2016; 6:194. Epub 2017/01/14. https://doi.org/10.3389/fcimb.2016.00194 PMID: 28083516; PubMed Central PMCID: PMC5186781.

39. Banemann A, Deppisch H, Gross R. The lipopolysaccharide of Bordetella bronchiseptica acts as a protective shield against antimicrobial peptides. Infect Immun. 1998; 66(12):5607–12. Epub 1998/11/24. https://doi.org/10.1128/IAI.66.12.5607-5612.1998 PMID: 9826332.

40. Jaiswal S, Pati NB, Dubey M, Padhi C, Sahoo PK, Ray S, et al. The O-antigen negative wbaV mutant of Salmonella enterica serovar Enteritidis shows adaptive resistance to antimicrobial peptides and elicits colitis in streptomycin pretreated mouse model. Gut Pathog. 2015; 7:24. Epub 2015/09/09. https://doi.org/10.1186/s13099-015-0070-4 PMID: 26346801; PubMed Central PMCID: PMC4559907.

41. Caroff M, Chaby R, Karibian D, Perry J, Deprun C, Szabo L. Variations in the carbohydrate regions of Bordetella pertussis lipopolysaccharides: electrophoretic, serological, and structural features. J Bacteriol. 1990; 172(2):1121–8. Epub 1990/02/01. https://doi.org/10.1128/jb.172.2.1121-1128.1990 PMID: 2298694.

42. Nguyen HTT, Nguyen TH, Otto M. The staphylococcal exopolysaccharide PIA—Biosynthesis and role in biofilm formation, colonization, and infection. Comput Struct Biotechnol J. 2020; 18:3324–34. Epub 2020/11/27. https://doi.org/10.1016/j.csbj.2020.10.027 PMID: 33240473; PubMed Central PMCID: PMC7674160.

43. Arciola CR, Campoccia D, Ravaioli S, Montanaro L. Polysaccharide intercellular adhesin in biofilm: structural and regulatory aspects. Front Cell Infect Microbiol. 2015; 5:7. Epub 2015/02/26. https://doi.org/10.3389/fcimb.2015.00007 PMID: 25713785; PubMed Central PMCID: PMC4322838.

44. Hernaez B, Alcami A. Virus-encoded cytokine and chemokine decoy receptors. Curr Opin Immunol. 2020; 66:50–6. Epub 2020/05/15. https://doi.org/10.1016/j.coi.2020.04.008 PMID: 32408109.

45. Bonecchi R, Garlanda C, Mantovani A, Riva F. Cytokine decoy and scavenger receptors as key regulators of immunity and inflammation. Cytokine. 2016; 87:37–45. Epub 2016/08/09. https://doi.org/10.1016/j.cyto.2016.06.023 PMID: 27498604; PubMed Central PMCID: PMC5414836.

46. Grachev AA, Gerbst AG, Gening ML, Titov DV, Yudina ON, Tsvetkov YE, et al. NMR and conformational studies of linear and cyclic oligo-(1—>6)-beta-D-glucosamines. Carbohydr Res. 2011; 346 (15):2499–510. Epub 2011/09/29. https://doi.org/10.1016/j.carres.2011.08.031 PMID: 21945383; PubMed Central PMCID: PMC3201778.

47. Anderson ES. Viability of, and transfer of a plasmid from, E. coli K12 in human intestine. Nature. 1975; 255(5508):502–4. Epub 1975/06/05. https://doi.org/10.1038/255502a0 PMID: 1094298.

48. Smith HW. Survival of orally administered E. coli K 12 in alimentary tract of man. Nature. 1975; 255 (5508):500–2. Epub 1975/06/05. https://doi.org/10.1038/255500a0 PMID: 1094297.

49. Wang JY, Hsueh PR, Wang JT, Lee LN, Yang PC, Luh KT. Recurrent infections and chronic colonization by an Escherichia coli clone in the respiratory tract of a patient with severe cystic bronchiectasis. J Clin Microbiol. 2000; 38(7):2766–7. Epub 2000/07/06. https://doi.org/10.1128/JCM.38.7.2766-2767.2000 PMID: 10878083; PubMed Central PMCID: PMC87025.

50. Sukumar N, Love CF, Conover MS, Kock ND, Dubey P, Deora R. Active and passive immunizations with Bordetella colonization factor A protect mice against respiratory challenge with Bordetella bronchiseptica. Infect Immun. 2009; 77(2):885–95. Epub 2008/12/10. IAI.01076-08 [pii] https://doi.org/10.1128/IAI.01076-08 PMID: 19064638.

51. Stainer DW, Scholte MJ. A simple chemically defined medium for the production of phase I Bordetella pertussis. J Gen Microbiol. 1970; 63(2):211–20. Epub 1970/10/01. https://doi.org/10.1099/00221287-63-2-211 PMID: 4324651.

52. Caution K, Yount K, Deora R, Dubey P. Evaluation of Host-Pathogen Responses and Vaccine Efficacy in Mice. J Vis Exp. 2019;(144). Epub 2019/03/12. https://doi.org/10.3791/58930 PMID: 30855568; PubMed Central PMCID: PMC7304499.